$[(\mathrm{en})\mathrm{Pt}(\mathrm{uracilate})]_4{}^{4+}$: A Metal Analogue of Calix[4]arene. Similarities and Differences with Classical Calix[4]arenes

Holger Rauter, Edda C. Hillgeris, Andrea Erxleben, and Bernhard Lippert*

Contribution from the Fachbereich Chemie, Universität Dortmund, D-44221 Dortmund, Germany

Received July 6, 1993[⊛]

Abstract: The preparation, X-ray crystal structure, and the solution behavior of a cyclic, tetranuclear nucleobase complex of $(\mathrm{en})\mathrm{Pt^{II}}$, $[(\mathrm{en})\mathrm{Pt}(\mathrm{UH}\text{-}N1,N3)]_4(\mathrm{NO_3})_4$ (**2**) (with en = 1.2-diaminoethane, UH = uracil monoanion, *N1*,*N3* = platination sites) is described. The tetranuclear cation of **2** displays close similarities with calix[4]arenes as far as overall geometry and conformational behavior is concerned. The affinity of the metal analogue **2** for metal cations appears to be more pronounced as compared to typical calix[4]arenes, however. In the solid state, **2** adopts a 1,3-alternate conformation of the four uracil rings, but in solution and after deprotonation to $[(\mathrm{en})\mathrm{Pt}(\mathrm{U}\text{-}N1,N3)]_4$ a second major species (cone conformer) occurs in solution. The assignment of this species is made on the basis of preliminary X-ray crystal data of a $\mathrm{Ag_4}$ derivative of **2**, $[(\mathrm{en})\mathrm{Pt}(\mathrm{UH})\mathrm{Ag}]_4(\mathrm{NO_3})_8\cdot 4\mathrm{H_2O}$ (**3**), in which the four uracil rings adopt a pinched-cone conformation and which, after $\mathrm{Ag^+}$ removal by means of $\mathrm{Cl^-}$, produces an identical species. **2** forms spontaneously in aqueous solution from the mononuclear precursor $[(\mathrm{en})\mathrm{Pt}(\mathrm{UH}\text{-}N1)(\mathrm{H_2O})](\mathrm{NO_3})\cdot\mathrm{H_2O}$ (**1**). The analogous *cis*-$[(\mathrm{NH_3})_2\mathrm{Pt}(\mathrm{UH}\text{-}N1)(\mathrm{H_2O})](\mathrm{NO_3})$ seems to behave similarly, although condensation products have not been isolated. In contrast, the N(3) linkage isomer *cis*-$[(\mathrm{NH_3})_2\mathrm{Pt}(\mathrm{UH}\text{-}N3)(\mathrm{H_2O})](\mathrm{NO_3})$, prepared *in situ* from *cis*-$(\mathrm{NH_3})_2\mathrm{Pt}(\mathrm{UH}\text{-}N3)\mathrm{Cl}\cdot 2\mathrm{H_2O}$ (**4**) and $\mathrm{AgNO_3}$, does not form a cyclic tetramer under comparable experimental conditions but dimerizes only to a *head–tail* species with *N3*,O Pt coordination and a μ-OH complex, depending upon pH. Crystallographic data for the three structurally characterized compounds **1**, **2**, and **4** are as follows: **1**, triclinic system, space group $P1$, $a = 7.229(1)$ Å, $b = 9.732(3)$ Å, $c = 9.968(2)$ Å, $\alpha = 107.37(2)°$, $\beta = 103.14(1)°$, $\gamma = 99.46(2)°$, $Z = 2$; **2**, tetragonal system, space group $P4(2)/n$, $a = 16.117(8)$ Å, $b = 16.131(8)$ Å, $c = 8.626(3)$ Å, $Z = 4$; **4**, monoclinic system, space group $P2(1)/c$, $a = 6.592(14)$ Å, $b = 20.135(25\ )$ Å, $c = 7.493(10)$ Å, $\beta = 92.32(14)°$, $Z = 4$. The cyclic tetramer **2** can be considered a prototype of a metal analogue of a calix[4]arene. Implications for the synthesis of other metal analogues of calixarenes and possible host–guest chemistry are briefly pointed out.

Classical calixarenes are cyclic condensation products of varying ring size derived from *para* substituted phenols and formaldehyde.[1,2] Modifications, either at the level of the phenol or the condensating agent or both, have led to a number of heterocalixarenes.[3] Interest in calixarenes primarily results from their ability to function as hosts for small molecules or ions as well as their metal binding properties, either in the cavity[4] or at the periphery ("lower rim").[5,6]

In this paper we report on the formation, the structure, and solution properties of a tetranuclear metal complex, $[(\mathrm{en})\mathrm{Pt}(\mathrm{uracilate}\text{-}N1,N3)]_4{}^{4+}$, which can be considered a special heterocalixarene, namely a metal analogue of a calix[4]arene. The bridging entity of the classical calix[4]arene, usually a $\mathrm{CH_2}$ group, is here replaced by a $(\mathrm{en})\mathrm{Pt^{II}}$ entity (Chart 1). This change, the replacement of the *p*-phenol by the 2,4-dioxopyrimidine and the positive charge introduced by the metal cations, leads to a number of differences as compared to the classical calix[4]arenes.

The title compound $[(\mathrm{en})\mathrm{Pt}(\mathrm{UH}\text{-}N1,N3)]_4{}^{4+}$ forms spontaneously from the mononuclear precursor $[(\mathrm{en})\mathrm{Pt}(\mathrm{UH}\text{-}N1)(\mathrm{H_2O})]^+$.[7] Our interest in uracil complexes of platinum relates to a class of oligomeric, mixed-valence compounds formed upon reaction of *cis*-$[(\mathrm{NH_3})_2\mathrm{Pt}(\mathrm{H_2O})_2]^{2+}$ and uracil ("platinum pyrimidine blues") or other cyclic amides.[8,9] X-ray crystallographic work on similar systems (α-pyridone,[10] 1-methyluracil,[11] α-pyrrolidone,[12] and acetamide[13]) has contributed much to the understanding of basic features of the blues. On the other hand, the coordination chemistry of underivatized uracil (thymine) is least well understood, due to the higher number of potential Pt binding site, e.g., N(1), N(3), O(2), O(4), and even C(5) and combinations thereof.

A preliminary report on the cyclic tetranuclear complex has appeared.[14]

[⊛] Abstract published in *Advance ACS Abstracts*, December 15, 1993.

(1) Gutsche, C. D. *Calixarenes*; Royal Society of Chemistry: Cambridge, 1989.

(2) *Calixarenes: A Versatile Class of Macrocyclic Compounds*; Böhmer, V.; Vicens, J.; Eds.; Kluwer: Dordrecht, 1991.

(3) See, e.g.: (a) Newkome, G. R.; Joo, Y. J.; Fronczek, F. R. *J. Chem. Soc., Chem. Commun.* **1987**, 854. (b) Pratt, J. A. E.; Sutherland, I. O.; Newton, R. F. *J. Chem. Soc., Perkin Trans.* **1988**, 13.

(4) (a) Hofmeister, G. E.; Hahn, F. E.; Pedersen, S. F. *J. Am. Chem. Soc.* **1989**, *111*, 2318. (b) Hofmeister. G. E.; Alvarado, E.; Leary, J. A.; Yoon, D. I.; Pedersen, S. F. *J. Am. Chem. Soc.* **1990**, *112*, 8843.

(5) See, e.g.: (a) Olmstead, M. M.; Sigel, G.; Hope, H.; Xu, X.; Power, P. P. *J. Am. Chem. Soc.* **1985**, *107*, 8087. (b) Bott, S. G.; Coleman, A. W.; Atwood, J. L. *J. Chem. Soc., Chem. Commun.* **1986**, 610. (c) Bott, S. G.; Coleman, A. W.; Atwood, J. L. *J. Am. Chem. Soc.* **1986**, *108*, 1709. (d) Coleman, A. W.; Bott, S. G.; Atwood, J. L. *J. Inclusion Phenom.* **1987**, *5*, 581. (e) Bott, S. W.; Coleman, A. W.; Atwood, J. L. *J. Inclusion Phenom.* **1987**, *5*, 747. (f) Furphy, B. M.; Harrowfield, J. M.; Kepert, D. L.; Skelton, B. W.; White, A. H.; Wilner, F. R. *Inorg. Chem.* **1987**, *26*, 4231. (g) Adreetti, G. D.; Calestani, G.; Ugozzoli, F.; Arduini, A.; Ghidini, E.; Pochini, A.; Ungaro, R. *J. Inclusion Phenom.* **1987**, *5*, 123. (h) Aoki, I.; Sakaki, T.; Shinkai, S. *J. Chem. Soc., Chem. Commun.* **1992**, 730.

(6) (a) Shinkai, S.: Koreishi, H.; Ueda, K.; Arimura, T.; Manabe, O. *J. Am. Chem. Soc.* **1987**, *109*, 6371. (b) Shinkai, S.; Shiramana, Y.; Satoh, H.; Manaba, O.; Arimura, R.; Fujimoto, K.; Matsuda, T. *J. Chem. Soc., Perkin Trans. 2* **1989**, 1167.

(7) Abbrevations used: $\mathrm{UH_2}$ = neutral uracil; UH = monoanion; U = dianion; –*N1* etc. denotes Pt binding site; en = 1,2-diaminoethane.

(8) (a) Davidson, J. P.; Faber, P. J.; Fischer, R. G.; Mansy, S.; Peresie, H. J.; Rosenberg, B.; VanCamp, L. *Cancer Chemother. Rep., Part 1* **1975**, *59*, 287. (b) Lippert, B. *J. Clin. Hematol. Oncol.* **1977**, *7*, 26.

(9) Lippert, B. *Inorg. Chem.* **1981**, *20*, 4326.

(10) (a) Barton, J. K.; Rabinowitz, H. N.; Szalda, D. J.; Lippard, S. J. *J. Am. Chem. Soc.* **1977**, *99*, 2827. (b) Barton, J. K.; Szalda, D. J.; Rabinowitz, H. N.; Waszczak, J. V.; Lippard, S. J. *J. Am. Chem. Soc.* **1979**, *101*, 1434.

(11) (a) Mascharak, P. K.; Williams, I. D.; Lippard, S. J. *J. Am. Chem. Soc.* **1984**, *106*, 6428. (b) O'Halloran, T. V.; Mascharak, P. K.; Williams, I. D.; Roberts, M. M.; Lippard, S. *J. Inorg. Chem.* **1982**, *26*, 1261. (c) Lippert, B.; Neugebauer, D. *Inorg. Chem.* **1982**, *21*, 451. (d) Lippert, B.; Schöllhorn, H.; Thewalt, U. *Inorg. Chem.* **1987**, *26*, 1736.

(12) Matsumoto, K.; Takahashi, H.; Fuwa, K. *J. Am. Chem. Soc.* **1984**, *106*, 2049 and references cited.

(13) (a) Sakai, K.; Matsumoto, K. *J. Am. Chem. Soc.* **1989**, *111*, 3074. (b) Matsumoto, K.; Sakai, K.; Nishio, K.; Tokisue, Y.; Ito, R.; Nishide, T.; Shichi, Y. *J. Am. Chem. Soc.* **1992**, *114*, 8110.

(14) Rauter, H.; Hillgeris, E. C.; Lippert, B. *J. Chem. Soc., Chem. Commun.* **1992**, 1385.

0002-7863/94/1516-0616$04.50/0

Chart 1

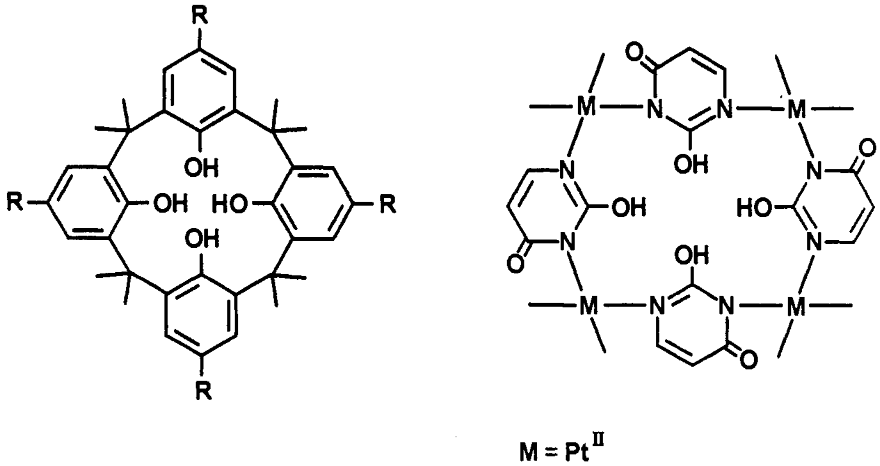

Chart 2

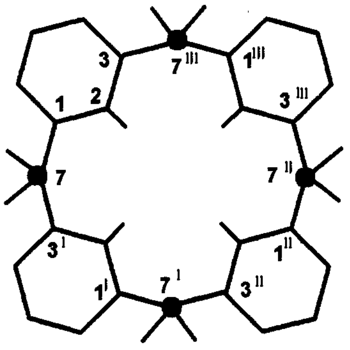

Experimental Section

Preparations. *cis*-$(NH_3)_2PtCl_2$,[15] (en)$PtCl_2$,[16] (en)Pt(UH-*N1*)-Cl·H_2O,[9] and *cis*-$(NH_3)_2$Pt(UH-*N1*)Cl[9] were prepared from K_2PtCl_4 (Degussa) and uracil (Fluka), respectively.

[(en)Pt(UH-*N1*)(H_2O)]NO_3·H_2O (**1**) was prepared in a similar way as described (compound B in ref 9). Crystallization at 4 °C (3–5 days) instead of room temperature gave better yields (maximum 160 mg, 35%, for a 1 mmol preparation), but the reported varying yields were confirmed. Elemental analysis data and IR spectra were identical with previously prepared samples.

[(en)Pt(UH-*N1*,*N3*)]$_4(NO_3)_4$ (**2**) was obtained in a similar way as reported (compound A in ref 9) or isolated from acidified (6 N HNO_3, pH ≈ 0) solutions after filtration of **1**. The yield of **2** after 5 days of crystallization was 117 mg for a 1 mmol preparation, corresponding to 27% based on Pt monomer. Elemental analysis data of single crystals of **2** (Found: C, 16.0; H, 2.6; N, 16.0) fit the description as dihydrate slightly better than as anhydrate, which is suggested on the basis of the X-ray analysis.

[(en)Pt(UH)Ag]$_4(NO_3)_8$·4H_2O (3) was obtained as follows: An aged solution of **1** (0.7 mmol, 5 mL of H_2O) was adjusted to pH 0 (6 N HNO_3), and 950 mg of $AgNO_3$ (8 equiv) was added. After filtration of some precipitate, the yellow solution was allowed to stand for 5 days at room temperature. After that time, colorless crystals had formed which were filtered and air dried (yield: 96 mg). Anal. Calcd for $[(C_2H_8N_2)_4Pt_4(C_4H_3N_2O_2)_4Ag_4](NO_3)_8\cdot4H_2O$: C, 11.7; H, 2.13; N, 13.6. Found: C, 11.5; H, 2.1; N, 13.5. Preliminary X-ray data: orthorhombric system; space group *Cmcm*, *a* = 15.069(3) Å, *b* = 19.997-(4) Å, *c* = 21.114(4) Å, *Z* = 4.

***cis*-$(NH_3)_2$Pt(UH-*N3*)Cl·2H_2O (4)**: *cis*-$(NH_3)_2PtCl_2$ (2.585 g) and UH_2 (0.965 g) were suspended in H_2O (500 mL). Stirring at 40 °C with the pH kept at 3.5–4.5 by means of KOH gave a brownish yellow solution. After 5 days, the solution was evaporated to dryness. The yellow-brown solid (3.308 g) was redissolved in H_2O and passed in small fractions over Sephadex G10. Only 58% of the material was recovered after elution with water (rest remained on the column), consisting of a mixture of species, including UH_2, *cis*-$(NH_3)_2PtCl_2$, *cis*-$(NH_3)_2$Pt(UH-*N3*)$_2$, and **4**. Compound **4** eluted between fractions containing the bis(uracil) compound and free uracil. The isolated yield of pure **4** was 6% only, but no attempts have been made to improve yields by purifying other fractions that contained **4**. IR (cm^{-1}) 312 m, 813 m, 1098 m, 1256 m, 1330 m, 1384 s, 1413 s, 1547 vs, 1625 vs, 1681 s, 3270 s. Anal. Calcd for $(NH_3)_2Pt(C_4H_3N_2O_2)Cl\cdot2H_2O$: C, 11.7; H, 3.2; N, 13.6. Found: C, 11.8; H, 3.2; N, 13.6.

Instrumentation. IR spectra (KBr pellets) were taken on Perkin-Elmer 580 B and Bruker IFs 113v FT spectrometers. ^1H NMR spectra were recorded on a Bruker AC 200 FT NMR spectrometer using D_2O with NMe_4^+ (3.18 ppm rel TMS) as internal reference and Me_2SO with TMS as internal standard. For aqueous solutions, pD values were determined by use of a glass electrode and addition of 0.4 to the pH meter reading (pH*). 2D-COSY spectra were recorded using standard procedures. Potentiometric titration of **2** and *cis*-[$(NH_3)_2$Pt(UH-*N3*)(H_2O)]$^+$ were carried out by use of an automated titroprocessor (Model 686, Metrohm) and a combination glass electrode.

X-ray Analysis. The following compounds were studied by single-crystal X-ray crystallography: [(en)Pt(UH-*N1*)(H_2O)]NO_3·H_2O (**1**), [(en)Pt(UH-*N1*,*N3*)]$_4(NO_3)_4$ (**2**), and *cis*-$(NH_3)_2$Pt(UH-*N3*)Cl·2H_2O (**4**). Unit cell dimensions were determined from 23 centered reflections ($4 \leq 2\theta \leq 19°$) for **1**, 21 reflections ($5 \leq 2\theta \leq 22°$) for **2**, and 11 reflections ($4 \leq 2\theta \leq 15°$) for **4**. Diffraction data were collected at room temperature using graphite-monochromated Mo Kα radiation (λ = 0.7107 Å) with a Siemens R3m/V (**1**) and a Nicolet R3m/V diffractometer (**2** and **4**). An empirical absorption correction was made for all data (ψ scans). The structures were solved by direct methods (**2**), Patterson (**1** and **4**), and Fourier methods applying the SHELXTL PLUS[17] program. Full matrix least-squares refinement (on F) was performed with anisotropic thermal parameters for non-H atoms and isotropic parameters for H atoms (**1** and **2**) using SHELXTL PLUS. Crystallographic data and details of the refinement are reported in Table 1. Positional and thermal parameters for **1**, **2**, and **4** are listed in Tables 2–4.

Results and Discussion

Solution Chemistry of [(en)Pt(UH-*N1*)(H_2O)]$^+$ and Spontaneous Formation of Pt_4. Treatment of (en)Pt(UH-*N1*)Cl, a derivative of the X-ray structurally characterized (en)Pt(UH-*N1*)Cl·(H_5O_2)Cl,[18] with 1 equiv of $AgNO_3$ produces [(en)Pt-(UH-*N1*)(H_2O)]$^+$. The species, which is identified by ^1H NMR spectroscopy immediately after dissolving crystalline [(en)Pt-(UH-*N1*)(H_2O)]NO_3·H_2O (**1**) in D_2O, undergoes rapid changes in solution with time (cf. Supplementary Material). These changes include the formation of a number of new uracil resonances (after several days at least 11 new sets) and eventually the complete isotopic exchange of uracil-H(5) to D(5) during this time. There are slight changes in ^1H NMR spectra depending

---

(15) (a) Dhara, S. G. *Indian J. Chem.* **1970**, *8*, 193. (b) Raudaschl, G.; Lippert, B.; Hoeschele, J. D.; Howard-Lock, H. E.; Lock, C. J. L.; Pilon, P. *Inorg. Chim. Acta* **1985**, *106*, 141.

(16) Basolo, F.; Bailar, J. C., Jr.; Tarr, B. R. *J. Am. Chem. Soc.* **1950**, *72*, 2433.

(17) Sheldrick, G. M. *SHELXTL PLUS (Release 3.4) for Nicolet R3m/v Crystallographic System*; University of Göttingen, F.R.G., 1987.

(18) Faggiani, R.; Lippert, B.; Lock, C. J. L. *Inorg. Chem.* **1980**, *19*, 295.

Table 1. Crystallographic Data and Details of Refinement of **1**, **2**, and **4** for Data Collected at 20 °C Using Mo Kα Radiation (λ = 0.7107 Å)

	1	**2**	**4**
formula	$C_6H_{11}N_5O_7Pt$	$C_{20}H_{44}N_{16}O_8Pt_4$	$C_4H_{13}N_4O_4PtCl$
fw g/mol	460.3	1417.0	411.7
crystal system	triclinic	tetragonal	monoclinic
space group	*P*1	*P*4(2)/n	*P*2(1)/c
crystal size, mm	0.02 × 0.016 × 0.026	0.15 × 0.15 × 0.62	0.048 × 0.064 × 0.096
a, Å	7.229(1)	16.117(8)	6.592(14)
b, Å	9.732(3)	16.131(8)	20.135(25)
c, Å	9.968(2)	8.626(3)	7.493(10)
α, deg	107.37(2)		
β, deg	103.14(1)		92.32(14)
γ, deg	99.46(2)		
V, Å^3	631.1(2)	2242.6(7)	993.7(2.8)
Z	2	4	4
d_{calc}, g cm^{-3}	2.422	2.54	2.645
μ(Mo Kα), cm^{-1}	11.26	12.6	14.37
F(000)	432	1600	736
scan	ω	$2\Theta/\omega$	$2\Theta/\omega$
2Θ range, deg	3–50	3–50	3–50
no. of reflcns measd	2424	4424	2449
no. of reflcns obsd	1876 ($F \geq 3\,\Theta\sigma(F)$)	1152 ($F \geq 2\Theta\sigma(F)$)	1054 ($F \geq 4\,\Theta\sigma(F)$)
R	3.72	5.13	5.28
R_w	3.44	5.25	5.25
good-of-fit	1.17	1.64	1.47
data to parameter ratio	10.7:1	7.4:1	8.6:1

Table 2. Atomic Coordinates and Equivalent Isotropic Displacement Coefficients (Å^2) for **1**

	x	*y*	*z*	*U*(eq)[a]
Pt(1)	0.2745(1)	0.1586(1)	0.1629(1)	0.027(1)
O(1)	0.2387(11)	−0.0689(8)	0.0805(7)	0.040(3)
N(1)	0.3483(12)	0.1494(9)	0.3674(8)	0.031(3)
C(2)	0.2103(14)	0.0938(10)	0.4213(9)	0.028(4)
O(2)	0.0359(9)	0.0345(8)	0.3422(7)	0.038(3)
N(3)	0.2638(11)	0.1008(9)	0.5641(8)	0.031(3)
C(4)	0.4481(14)	0.1577(11)	0.6603(9)	0.032(4)
O(4)	0.4773(10)	0.1567(8)	0.7892(6)	0.042(3)
C(5)	0.5952(14)	0.2078(11)	0.5999(9)	0.032(4)
C(6)	0.5357(14)	0.2046(11)	0.4601(10)	0.031(4)
N(21)	0.3037(13)	0.3792(9)	0.2397(9)	0.040(4)
C(21)	0.2574(36)	0.4307(17)	0.1154(13)	0.135(11)
C(22)	0.2077(31)	0.3354(14)	−0.0202(13)	0.108(10)
N(22)	0.2000(12)	0.1792(10)	−0.0398(8)	0.038(4)
N(10)	0.1494(20)	0.4471(13)	0.6236(16)	0.067(6)
O(11)	0.2816(19)	0.4584(15)	0.5662(16)	0.121(8)
O(12)	0.0044(19)	0.3497(16)	0.5562(22)	0.172(11)
O(13)	0.1753(39)	0.5285(17)	0.7409(16)	0.222(17)
Ow	0.7903(12)	0.1768(9)	0.1976(7)	0.055(4)

[a] Equivalent isotropic *U* defined as one-third of the trace of the orthogonalized U_{ij} tensor.

Table 3. Atomic Coordinates and Equivalent Isotropic Displacement Coefficients (Å^2) for **2**

	x	*y*	*z*	*U*(eq)[a]
Pt(1)	0.1563(0)	0.0116(0)	0.2167(0)	0.0641(3)
O(2)	0.3274(7)	0.0628(6)	0.3555(17)	0.068(5)
O(4)	0.435(1)	0.211(1)	−0.052(2)	0.13(8)
O(11)	0.120(1)	0.578(1)	0.084(2)	0.16(10)
O(12)	0.1610(14)	0.6527(9)	0.2567(24)	0.13(9)
O(13)	0.040(1)	0.603(1)	0.284(2)	0.127(9)
N(1)	0.2552(8)	0.0728(7)	0.1269(19)	0.06(6)
N(3)	0.3885(7)	0.1314(8)	0.1467(18)	0.063(7)
N(10)	0.106(2)	0.611(1)	0.205(3)	0.11(12)
N(21)	0.1814(10)	−0.0923(8)	0.0918(17)	0.08(7)
N(22)	0.053(1)	−0.052(1)	0.289(2)	0.095(7)
C(2)	0.326(1)	0.085(1)	0.221(2)	0.06(7)
C(4)	0.382(1)	0.159(1)	0.006(2)	0.06(7)
C(5)	0.315(1)	0.139(1)	−0.085(2)	0.09(9)
C(6)	0.247(1)	0.100(1)	−0.025(3)	0.10(10)
C(21)	0.121(2)	−0.152(1)	0.146(3)	0.14(15)
C(22)	0.040(2)	−0.121(2)	0.182(3)	0.16(16)

[a] Equivalent isotropic *U* defined as one-third of the trace of the orthogonalized U_{ij} tensor.

Table 4. Atomic Coordinates and Equivalent Isotropic Displacement Coefficients (Å^2) for **4**

atom	*x*	*y*	*z*	*U*(eq)[a]
Pt(1)	0.0339(2)	0.20313(4)	0.3268(1)	0.267(3)
Cl(1)	0.3452(11)	0.1718(3)	0.4410(9)	0.424(23)
N(11)	0.1372(28)	0.2980(9)	0.3272(21)	0.366(60)
C(4)	−0.1655(34)	0.0917(10)	0.4867(25)	0.182(49)
N(3)	−0.0810(29)	0.1093(9)	0.3374(23)	0.278(63)
O(4)	−0.1812(26)	0.1285(7)	0.6140(19)	0.359(58)
O(2)	0.0477(32)	0.0833(8)	0.0678(18)	0.476(70)
N(10)	−0.2364(27)	0.2304(8)	0.2197(19)	0.225(56)
N(1)	−0.1213(32)	0.0050(10)	0.2146(25)	0.357(76)
C(5)	−0.2585(36)	0.0242(10)	0.4927(28)	0.257(84)
C(6)	−0.2199(39)	−0.0161(12)	0.3588(31)	0.351(97)
C(2)	−0.0450(45)	0.0689(11)	0.1996(31)	0.331(82)
O1W	0.4038(35)	0.8531(10)	0.0893(26)	0.750(91)
O2W	0.4279(43)	0.0562(15)	0.1275(34)	0.141(15)

[a] Equivalent isotropic *U* defined as one-third of the trace of the orthogonalized U_{ij} tensor.

on whether some base had been added initially (pD 6) or not (pD $\sim$ 3, $c_{Pt} \approx 0.07$ M). In all cases, the pD drops with time (e.g., sample pD 6 by 4 pH units, sample pD 3 by 1 pH unit). Condensation reactions leading to dinuclear, μ-OH bridged species (Chart 3, A) or cyclic or open U-*N1*,*N3* bridged species (B) would in principle account for the observed drop in pH, while condensation via N(1),O(2) (or N(3),O(4) or N(3),O(2)) would not generate acidic protons, unless this binding mode causes a tremendous acidification of the remaining uracil NH proton (C). H(6) uracil resonances of the various species are spread out over a 0.6-ppm range. We can, at present, only assign two of the resonances safely, that of the monomer **1** and that of the cyclic tetramer **2**. Relative intensities of the signals due to **2** are in reasonable agreement with the isolated yield of the cyclic tetramer. If different conformers are allowed (*vide infra*), additional resonances might be accounted for. On the basis of model building, other cyclic structures are feasible, e.g., 3mers, 5mers, 6mers... Open structures will cause multiple uracil resonances due to nonequivalence of N(1) and N(3) bound terminal uracils and possibly also because of hindered rotations about Pt–N(uracil) bonds. Using two-dimensional NMR techniques (not shown), the correlation of H(5) and H(6) resonances can be achieved, but assignment of species other than **1** and **2** has not been possible.

Solution Behavior of [(en)Pt(UH-*N1*,*N3*)]$_4^{4+}$ (2). The ^{1}H NMR spectrum of **2** in Me_2SO-d_6 immediately after dissolving is very simple. Resonances are observed at 10.63 ppm (OH),

Scheme 1

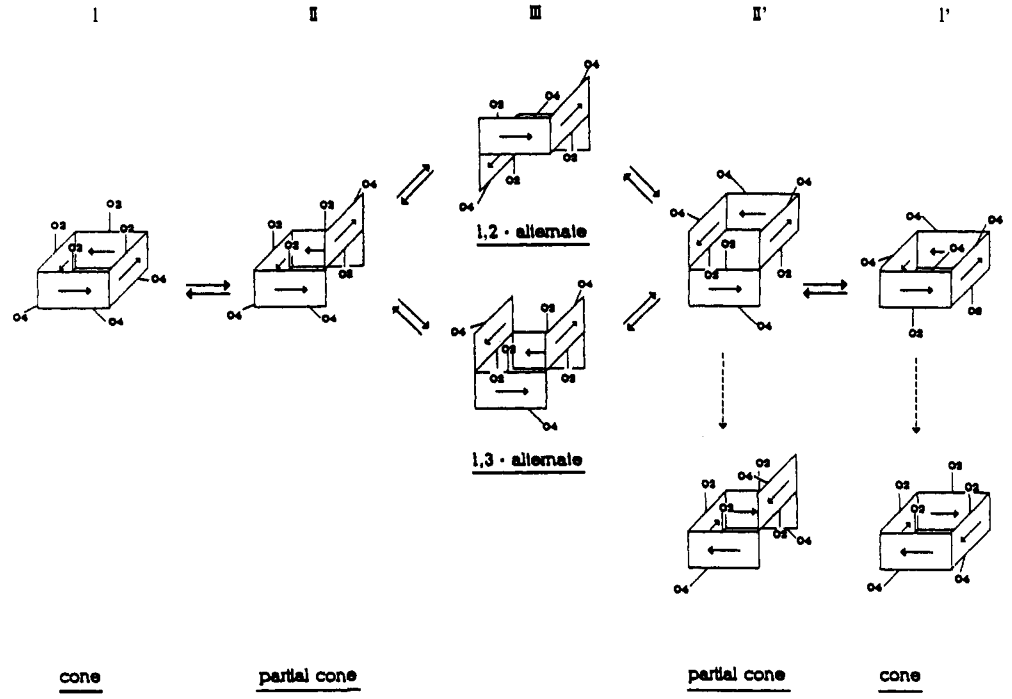

Chart 3

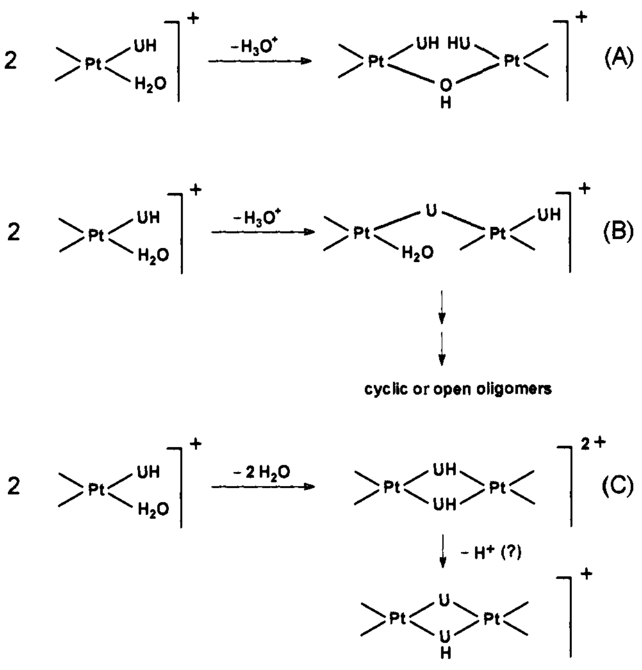

7.32 ppm (d, $^3J \sim 7.1$ Hz; H(6)), 5.98 and 6.11 ppm (NH_2), 5.32 and 5.33 ppm (d each; H(5)), and 3.32 ppm (CH_2), with relative intensities consistent with the assignment.

^{1}H NMR spectra recorded in D_2O are more complex in that (i) additional uracil resonances are observed, the formation of which is pH and time dependent, (ii) all uracil resonances display a pronounced pH dependence in their chemical shifts, and (iii) isotopic H → D exchange at the C(5) position occurs in acidic medium (*vide infra*).

The additional uracil resonances are *not* due to ^{195}Pt satellites, as typically found for H(5) and H(6) protons in N(1),N(3) bridged uracil complexes of Pt(II),[9] when spectra are recorded at 60 MHz.[19] Rather, we assign these resonances to conformers other than that of **2**, which is of C_2 symmetry (1,3-alternate) in the solid state. Before discussing arguments in support of this interpretation, a brief comparison with calix[4]arenes is of help.

Ring Flexibility in 2 and Comparison with Calix[4]arenes. According to Gutsche,[1] calix[4]arenes can exist in four principal conformations named cone, partial cone, 1,2-alternate, and 1,3-alternate conformation. Recently, an additional special form of the cone conformer, the "pinched cone" conformer, has been demonstrated to occur,[20] as predicted by theoretical calculations.[21] Although calix[4]arenes seem to prefer the cone conformation in the solid state, ^{1}H NMR spectroscopy has proven that at higher temperature interconversion of opposite cone conformers takes place[22] with partial and alternate conformers being intermediates.[21,22b] The energy barrier of the ring inversion shows a considerable solvent dependency.

From model building with **2** it is evident that conformers analogous to those of calix[4]arenes are feasible with our tetranuclear uracil complex as well. The solid-state structure of **2** then corresponds to the 1,3-alternate conformation which has rarely been observed experimentally for simple calix[4]arenes, however.[23] Ultimate proof for conformational flexibility of **2** comes from a mixed Pt_4Ag_4 complex **3** obtained by crystallization of **2** in the presence of $AgNO_3$. According to preliminary X-ray data, the four uracil rings adopt a pinched cone conformation in this mixed-metal compound. Unfortunately, we are unable at present to provide full crystallographic data on $[(en)Pt(UH)Ag]_4(NO_3)_8 \cdot 4H_2O$ (**3**) due to severe problems with the refinement of NO_3^- anions and water molecules. The octanuclear cation (supplementary material) proves the pinched cone conformation beyond doubt, however. Precipitation of all four Ag^I by means of Cl^- leads to an intact $Pt_4(UH)_4$ ring with uracil resonances in

---

(19) At 200 MHz, ^{195}Pt satellites are usually broadened beyond resolution, see: Lallemand, J.-Y.; Soulie, J.; Chottard, J.-C. *J. Chem. Soc., Chem. Commun.* **1980**, 438.

(20) Conner, M.; Janout, V.; Regen, S. L. *J. Am. Chem. Soc.* **1991**, *113*, 9670.

(21) Grootenhuis, P. D. J.; Kollman, P. A.; Groenen, L. C.; Reinhoudt, D. N.; van Hummel, G. J.; Ugozzoli, F.; Andreetti, G. D. *J. Am. Chem. Soc.* **1990**, *112*, 4165.

(22) (a) Shinkai in ref. 2, p. 173. (b) Groenen, L. C.; van Loon, J.-D.; Verboomm, W.; Harkema, S.; Casnati, A.; Ungaro, R.; Pochini, A.; Ugozzoli, F.; Reinhoudt, D. N. *J. Am. Chem. Soc.* **1991**, *113*, 2385.

(23) With suitable substituted calix[4]arenes, the 1,3-alternate conformation can be forced. See, e.g.: (a) Pappalardo, S.; Bottino, F.; Ronsisvalle, G. *Phosphorus Sulfur* **1984**, *19*, 327. (b) Ghidini, E.; Ugozzoli, F.; Ungaro, R.; Harkema, S.; El-Fadl, A. A.; Reinhoudt, D. N. *J. Am. Chem. Soc.* **1990**, *112*, 6979.

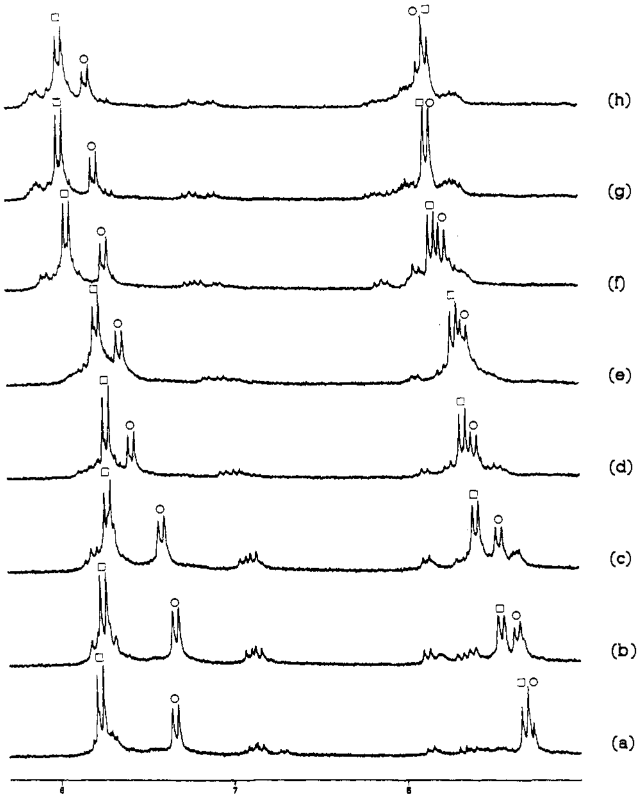

Figure 1. pH* dependent ^{1}H NMR spectra (D_2O, aromatic region only) of **2**: (a) After keeping the sample at pH* ≈ 8.5, 40 °C for 12 h. The intense doublets at 5.31 (H(5)) and 7.77 ppm (H(6)) are due to **2** in its 1,3-alternate conformation (□). The second most intense signal set (○) is assigned to the cone conformer of **2**. Other, minor resonances are not assigned; (b) pH* = 5.3; (c) pH* = 4.6; (d) pH* = 3.7; (e) pH* = 3.0; (f) pH* = 1.6; (g) pH* = 0.6; (h) pH* = 0.

the ^{1}H NMR that are distinctly different from those of **2** at identical pH. The gradual appearance of identical resonances after dissolving single crystals of **2** in D_2O clearly establishes that an interconversion between the 1,3-alternate form and the cone form takes place in solution. The other, minor uracil resonances observed in the ^{1}H NMR could in fact be due to the partial cone and/or 1,2-alternate forms.

In Scheme 1 possible ways of interconversion of the various conformers are schematically depicted. As evident, a complete conversion of one cone form to the other leads to a simultaneous reversal of the sense of orientation of the O(4) oxygens. This is a consequence of the substituent in 4-position of uracil as compared to 5-substituted phenols or aromatic rings identically substituted at the 4- and 6-positions. It is noted that the Pt_4Ag_4 complex contains these two forms of the cone conformer in a 1:1 ratio.

Acid/Base Equilibria of 2. The four acidic protons of **2** can be titrated with base. In the potentiometric titration curve only two neutralization steps are observed, after addition of two and four equivalents of OH^- per Pt, respectively. The previously reported pK_a values[9] have been confirmed, even though they originally had been attributed to the titration of two acidic protons of an assumed dimer. The reported pK_a values of *ca.* 2.6 and 5.7 thus are averaged over two individual dissociation processes each.

pH* dependent ^{1}H NMR spectra of freshly dissolved **2** are roughly consistent with these pK_a values, even though pH* dependence is not equally pronounced for the two uracil protons. There are at least two aspects of this study that deserve mentioning. First, the neutral cyclic tetramer $[(en)Pt(U\text{-}N1,N3)]_4$, which is present in solution above pH 8, is very soluble in water. This is surprising at first glance and suggests that it has undergone alkali adduct formation, e.g., $\{Na_x[(en)Pt(U\text{-}N1,N3)]_4\}(NO_3)_x$, with Na^+ coordinated through exocyclic oxygens. Considering the affinity of **2** for other metal ions[24] and similar findings with di- and polynuclear complexes of N(3) metalated 1-methyluracil and 1-methylthymine,[25] this is no longer unusual. Second, upon gentle heating (40 °C, 12 h) of a solution of **2** at pH* ≈ 8.5, additional sets of uracil resonances form at the expense of that of **2**. The most intense new set (Figure 1) which, upon titration with acid displays a pH* dependence different from that of **2** (Figure 2), is assigned to the cone conformer. At a given pH*, its chemical shift agrees with that of the Pt_4Ag_4 species **3** after addition of Cl^-. H(5), but in particular H(6), occurs upfield in the cone conformer, which most likely is due to the more efficient ring current effects of the *cis*-positioned uracil rings in the cone form as compared to the 1,3-alternate form. As is to be seen from Figure 3, the two conformers have somewhat different H^+ affinities (acidities). This is probably a consequence of different protonation sites, *viz.* O(4)H···O(2) in **2**, but a cyclic arrangement with four O(2) oxygens protonated and acting both as H donors and acceptors in the cone conformer. The situation thus is analogous to that in Pt_4Ag_4 with Ag^+ replaced by H^+. In the cone arrangement, the O(4) sites eventually might also become protonated, without stabilization through an intramolecular H bond. These protons should therefore be very acidic (pK_a estimated ≤0).

Table 5. Selected Interatomic Distances (Å), Angles (deg), and Hydrogen-Bonding Interactions for **1**

	Distances		
Pt(1)–O(1')	2.067(7)	Pt(1)–N(1)	2.019(8)
Pt(1)–N(21)	2.009(9)	Pt(1)–N(22)	2.049(9)
N(1)–C(2)	1.347(14)	N(1)–C(6)	1.369(11)
C(2)–O(2)	1.258(10)	C(2)–N(3)	1.366(12)
N(3)–C(4)	1.364(10)	C(4)–O(4)	1.257(12)
C(4)–C(5)	1.424(15)	C(5)–C(6)	1.350(14)
N(21)–C(21)	1.461(19)	C(21)–C(22)	1.319(16)
C(22)–N(22)	1.463(17)	N(10)–O(11)	1.226(23)
N(10)–O(12)	1.192(16)	N(10)–O(13)	1.153(19)
	Angles		
O(1)–Pt(1)–N(1)	88.4(3)	O(1)–Pt(1)–N(21)	178.7(3)
N(1)–Pt(1)–N(21)	92.6(3)	O(1)–Pt(1)–N(22)	94.6(3)
N(1)–Pt(1)–N(22)	177.1(3)	N(21)–Pt(1)–N(22)	84.5(4)
Pt(1)–N(1)–C(2)	120.6(6)	Pt(1)–N(1)–C(6)	122.6(7)
C(2)–N(1)–C(6)	116.7(8)	N(1)–C(2)–O(2)	121.3(8)
N(1)–C(2)–N(3)	118.7(8)	O(2)–C(2)–N(3)	120.0(9)
C(2)–N(3)–C(4)	126.1(9)	N(3)–C(4)–O(4)	119.6(9)
N(3)–C(4)–C(5)	114.8(8)	O(4)–C(4)–C(5)	125.5(8)
C(4)–C(5)–C(6)	117.3(8)	N(1)–C(6)–C(5)	126.2(10)
Pt(1)–N(21)–C(21)	109.0(7)	N(21)–C(21)–C(22)	120.0(14)
C(21)–C(22)–N(22)	117.7(13)	Pt(1)–N(22)–C(22)	108.8(6)
O(11)–N(10)–O(12)	117.9(15)	O(11)–N(10)–O(13)	118.0(17)
O(12)–N(10)–O(13)	124.1(22)		
	Possible Hydrogen Bond Distances ≤3 Å		
N(3)–O(2)[h]	2.830(11)	N(22)–O(4)[d]	2.905(11)
O(1)–O(4)[b]	2.581(11)	O(1)–O(W)[e]	2.601(9)
O(2)–O(W)[c]	2.822(11)	O(13)–O(W)[f]	2.708(19)
	Possible Hydrogen Bond Angles		
C(2)–N(3)–O(2)[h]	115.6(6)	C(2)–O(2)–N(3)[a]	124.3(6)
Pt(1)–N(22)–O(4)[d]	119.3(4)	C(4)–O(4)–N(22)[g]	126.6(7)
Pt(1)–O(1)–O(4)[b]	113.3(3)	C(4)–O(4)–O(1)[b]	123.9(7)
Pt(1)–O(1)–O(W)[e]	114.6(4)	C(2)–O(2)–O(W)[c]	125.0(7)
N(10)–O(13)–O(W)[f]	122.6(12)		

[a] Symmetry operations. [b] $1 - x, -y, 1 - z$. [c] $-1 + x, y, z$. [d] $x, y, -1 + z$. [e] $1 - x, -y, -z$. [f] $1 - x, 1 - y, 1 - z$. [g] $x, y, 1 + z$. [h] $-x, -y, 1 - z$.

Analogy of 1 with *cis*-$[(NH_3)_2Pt(UH\text{-}N1)(H_2O)]^+$. The aqueous chemistry of the aqua species of *cis*-$(NH_3)_2Pt(UH\text{-}N1)$-Cl is of similar complexity as that of **1**.[9] From comparison with **1** we are convinced that a cyclic tetramer in the 1,3 alternate

---

[24] Rauter, H.; Mutikainen, I.; Bolmberg, M.; Lock, C. J. L.; Lippert, B., submitted for publication.

[25] For alkali adducts see, e.g.: (a) Guay, F.; Beauchamp, A. *Inorg. Chim. Acta* **1982**, *66*, 57. (b) Renn, O.; Mutikainen, I.; Lippert, B., to be submitted. (c) Micklitz, W.; Lippert, B.; Lianza, F.; Albinati, A., to be submitted.

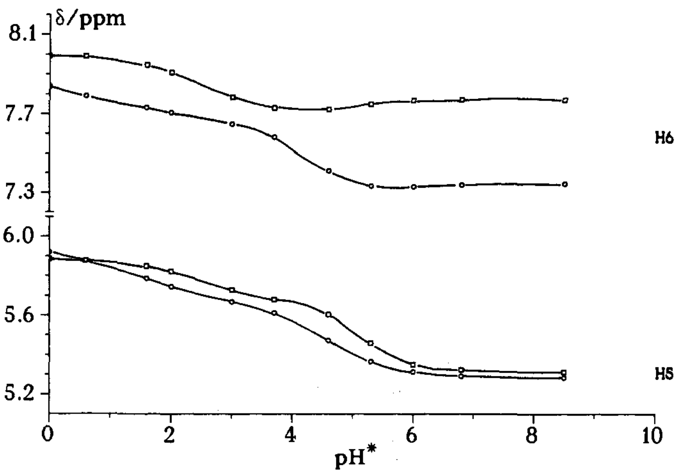

Figure 2. ^{1}H NMR chemical shifts of uracil H(5) and H(6) resonances of the two most intense conformers (1,3-alternate (□) and cone, (○)) of **2** between $0 \le pH^* \le 8.5$. When **2** in its 1,3-alternate conformation is dissolved (acidic pH) and rapidly titrated with strong acid or base, only the set of resonances due to the 1,3-alternate conformer (□) is observed.

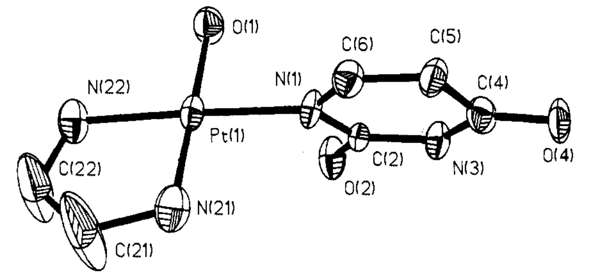

Figure 3. View of the cation of [(en)Pt(UH-*N1*)(H_2O)](NO_3)·H_2O (**1**) with atom numbering scheme.

conformation is also formed, although in lower yield. The intense ^{1}H NMR resonance for uracil-H(6) at 8.05 ppm, which is furthest downfield and occurs in the range of H(6) of **2**, is tentatively assigned to this species. We have not been able to isolate such a compound nor any of the other products, however. We found that, unlike with **1**, addition of HNO_3 to an aged solution of *cis*-[$(NH_3)_2$Pt(UH-*N1*)(H_2O)]$^+$ ($pH^* = 0$) causes a rapid change in color from pale yellow to dark brown and a complete broadening of the uracil resonances.

Crystal Structure Analysis of [(en)Pt(UH-*N1*)(H_2O)]NO_3·H_2O (1). The cation of **1** is shown in Figure 3. Selected interatomic distances and angles are given in Table 5. The compound represents one of very few examples of X-ray structurally characterized Pt^{II}–aqua complexes. Another example is the 1-methylcytosine (1-MeC) compound *cis*-[$(NH_3)_2$Pt(1-MeC-*N3*)(H_2O)]$(NO_3)_2$·H_2O.[26] The Pt–OH_2 distance in **1** (2.067(7) Å) compares well with the 2.052(8) Å distance in the 1-MeC compound. Other structural details of the Pt coordination geometry, the en and the uracil ligands are not unusual. The dihedral angle between the Pt plane and the uracil ring is 74.0°. As evident from a stereoview (supplementary material), uracil ligands of adjacent cations are H bonded via N(3)H and O(2) in pairs (2.830(11) Å). Pairs of such dimers are oriented in such a way, that uracil rings overlap partly. This stacking interaction is reinforced by pairs of strong H bonds (2.581(11) Å) between uracil–O(4) and the aqua ligand O(1).

X-ray Structure of [(en)Pt(UH-*N1,N3*)]$_4$(NO_3)$_4$ (2). A brief account on the solid-state structure of **2** has been published.[14] Figure 4 gives a view of the tetranuclear cation. Interatomic distances and angles are listed in Table 6. Four (en)Pt^{II} entities, which occupy the corners of a square (Pt(1)···Pt(1a), 5.86 Å), bridge four uracil rings in a way that each Pt is bound to N(1) of one ring and N(3) of a second one. The uracil ligands represent diplatinated rare tautomer forms of the uracil monoanion, with the acidic proton (normally at N(1) or N(3)) bound either at O(2) or O(4). The quality of the X-ray data does not permit a distinction. The exocyclic oxygens of the uracil ligands are arranged in a 1,3-alternating fashion, with O(2)s of two opposite rings being on the same side relative to the Pt_4 plane, while O(2)s of the two other rings are on the same but opposite sides of the Pt_4 framework. As a consequence, O(2) and O(4) oxygens of adjacent uracil rings are next to each other, connected by a strong H bond (2.53(2) Å) between the enol and the carbonyl group. This strong H bond probably accounts for the fact that the four uracil rings are not exactly perpendicular to the Pt_4 square but tilted in such a fashion as to make access to the inner cavity from top and bottom somewhat more difficult. Thus, C(5) atoms of opposite uracil rings (e.g., ring *a* and ring *b*) get closer to each other (4.14 Å) as compared to an expected value of 5.86 Å if the two rings were perpendicular to the Pt_4 square. Simultaneously, the separation between opposite O(2) sites (e.g., O(2a) and O(2b)) increases to 6.53 Å.

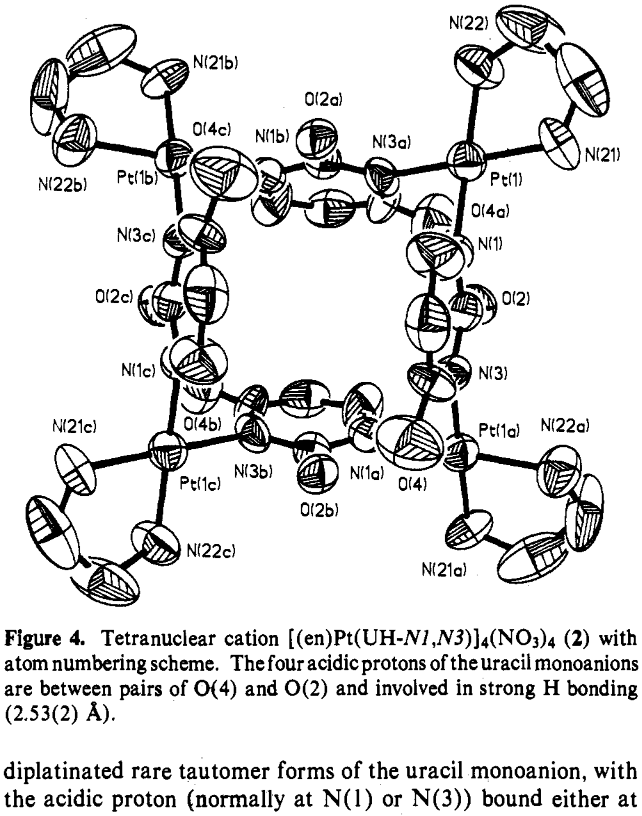

Figure 4. Tetranuclear cation [(en)Pt(UH-*N1,N3*)]$_4$(NO_3)$_4$ (**2**) with atom numbering scheme. The four acidic protons of the uracil monoanions are between pairs of O(4) and O(2) and involved in strong H bonding (2.53(2) Å).

The coordination geometry about the Pt^{II} is normal square-planar with slight deviations of angles. Pt–N distances are normal.

---

(26) Britten, J. F.; Lippert, B.; Lock, C. J. L.; Pilon, P. *Inorg. Chem.* **1982**, *21*, 1936.

Table 6. Selected Interatomic Distances (Å), Angles (deg), and Hydrogen-Bonding Interactions for **2**[a]

	Distances		
Pt(1)–N(3A)	2.036(14)	Pt(1)–N(21)	2.033(14)
Pt(1)–N(1)	2.028(14)	Pt(1)–N(22)	2.052(18)
N(1)–C(2)	1.419(24)	N(1)–C(6)	1.391(29)
C(2)–O(2)	1.211(25)	C(2)–N(3)	1.408(23)
N(3)–C(4)	1.299(25)	C(4)–O(4)	1.286(26)
C(4)–C(5)	1.381(29)	C(5)–C(6)	1.354(31)
N(21)–C(21)	1.454(33)	N(22)–C(22)	1.463(34)
C(21)–C(22)	1.435(43)	O(11)–N(10)	1.193(32)
O(13)–N(10)	1.274(36)	O(12)–N(10)	1.200(35)
	Angles		
N(3A)–Pt(1)–N(22)	93.3(5)	N(3A)–Pt(1)–N(21)	176.6(4)
N(3A)–Pt(1)–N(1)	89.5(4)	N(21)–Pt(1)–N(22)	85.0(6)
N(1)–Pt(1)–N(22)	175.2(6)	N(1)–Pt(1)–N(21)	92.4(6)
Pt(1)–N(1)–C(6)	116.3(12)	Pt(1)–N(1)–C(2)	118.8(12)
Pt(1)–N(21)–C(21)	104.0(14)	Pt(1)–N(22)–C(22)	107.8(15)
C(2)–N(1)–C(6)	124.9(15)	C(2)–N(3)–C(4)	123.8(15)
O(2)–C(2)–N(1)	121.4(17)	N(1)–C(6)–C(5)	115.5(20)
N(1)–C(2)–N(3)	112.8(16)	O(2)–C(2)–N(3)	125.6(17)
O(4)–C(4)–N(3)	122.4(18)	N(3)–C(4)–C(5)	120.6(17)
O(4)–C(4)–C(5)	116.8(18)	C(4)–C(5)–C(6)	121.9(20)
N(21)–C(21)–C(22)	116.6(21)	N(22)–C(22)–C(21)	105.5(23)
O(12)–N(10)–O(13)	118.6(24)	O(11)–N(10)–O(13)	125.7(25)
O(11)–N(10)–O(12)	115.7(27)		
	Possible Hydrogen Bond Distances		
O(2)–O(4)[f]	2.53(2)	N(21)–O(12)[b]	3.13(2)
N(21)–O(13)[b]	3.06(2)	N(21)–O(11)[c]	3.21(3)
N(21)–O(12)[c]	3.07(3)	N(22)–O(13)[e]	2.98(3)
N(22)–O(11)[d]	2.80(2)		
	Possible Hydrogen Bond Angles		
C(2)–O(2)–O(4)[f]	128.4(12)	C(4)–O(4)–O(2)[e]	103.3(13)
Pt(1)–N(21)–O(12)[b]	138.8(8)	C(21)–N(21)–O(13)[b]	100.6(14)
C(21)–N(21)–O(11)[c]	136.5(14)	Pt(1)–N(21)–O(12)[c]	100.4(6)
Pt(1)–N(22)–O(13)[e]	111.7(7)	Pt(1)–N(22)–O(11)[d]	111.0(8)

[a] Symmetry operations. [b] $-^1/_2 + y, -x, -^1/_2 + z$. [c] $^1/_2 - x, ^1/_2 - y, z$. [d] $-^1/_2 + y, -x, ^1/_2 + z$. [e] $^1/_2 - y, x, ^1/_2 - z$. [f] $y, ^1/_2 - x, ^1/_2 - z$.

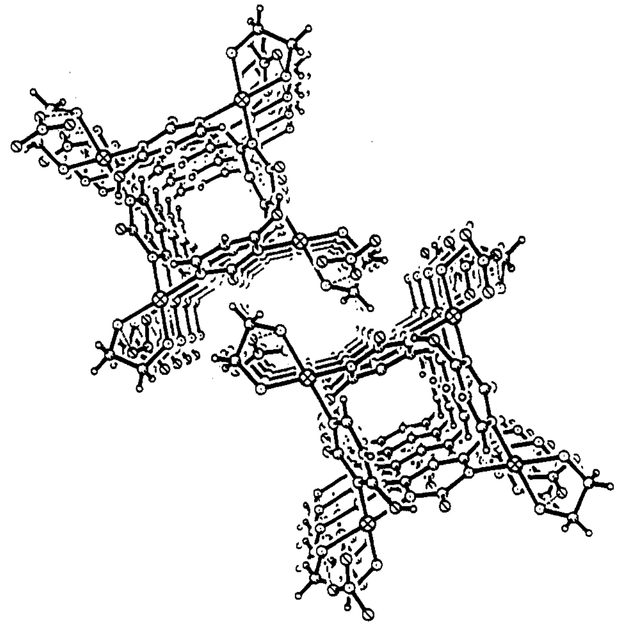

Figure 5. Packing of tetranuclear cations and nitrate anions in **2**. The view is along the *z*-axis. Nitrates link tetranuclear entities via en groups along this axis (supplementary material).

A discussion of the uracil geometry is not meaningful considering the relatively large errors.

In the crystal, tetranuclear cations are stacked along the *z*-axis, thereby producing long channels (Figure 5). Repeating units are 8.63 Å apart. As shown in the supplementary material, nitrate anions connect the cations via H bonds involving the NH_2 groups of the en ligands in the z-direction. (O(11)···N(22), 2.80(2) Å; O(12)···N(21), 3.13(2) Å, O(13)···N(21), 3.06(2) Å). At the same time (not shown), these nitrates also H bond to neighboring stacks, again to the amino groups of the en chelate rings (O(11)···N(21), 3.21(3) Å; O(12)···N(21), 3.07(3) Å; O(13)···N(22), 2.98(3) Å). As a result, each nitrate oxygens forms two H bonds, the two protons of N(22) are H bonded to one oxygen each, while each of the two amino protons of N(21) exhibits a bifurcated H bond to two nitrate oxygens.

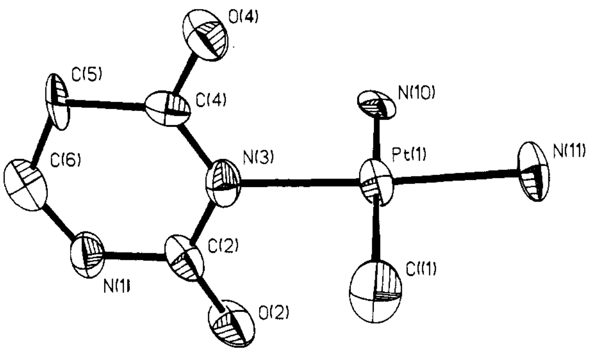

Figure 6. View of *cis*-$(NH_3)_2Pt(UH\text{-}N3)Cl\cdot 2H_2O$ (**4**) with atom numbering scheme.

Comparison with cis-$[(NH_3)_2Pt(UH\text{-}N3)(H_2O)]^+$ and X-ray Structure of *cis*-$(NH_3)_2Pt(UH\text{-}N3)Cl\cdot 2H_2O$ (4). We have prepared compound **4**, which contains the unsubstituted uracil monoanion bound to Pt(II) through N(3) in an attempt to synthesize the cyclic tetramer of the analogous *cis*-$(NH_3)_2Pt^{II}$ via an alternative route, starting with the N(3) linkage isomer.

Formation of **4** takes place surprisingly easily in moderately acidic aqueous solution (pH 3.5–4.5), well below the pK_a of uracil (*ca.* 9.5). According to ^{1}H NMR spectroscopy, reaction between *cis*-$(NH_3)_2PtCl_2$ and uracil leading to the N(3) linkage isomer is slow but remarkably efficient.[27] Specifically, there is no formation whatsoever of any species containing N(1) coordinated uracil. This situation contrasts the preferential formation of the N(1) linkage isomer from *cis*-$[(NH_3)_2PtCl(DMF)]^+$ and K^+UH^- in DMF.[9,28] Formation of **4** probably occurs via condensation of neutral uracil with a Pt(OH) hydrolysis species (cf. p$K_a \approx 6.4$ for *cis*-$[(NH_3)_2PtCl(H_2O)]^+$ or p$K_{a1} \approx 5.4$ for *cis*-$[(NH_3)_2Pt(H_2O)_2]^{2+}$ [29]).

The molecule *cis*-$(NH_3)_2Pt(UH\text{-}N3)Cl$ (**4**) is shown in Figure 6. Salient structural features are listed in Table 7. The compound represents the first X-ray structurally characterized example of a complex containing a uracil monoanion bound to a metal through N(3). The remaining acidic proton could not be located. Arguments concerning the site of protonation (N(1) or O(2)) which are based on consideration of the size of the internal ring angle at N(1)[30–32] cannot be applied due to the large errors. Likewise, a comparison of uracil geometries of N(1) and N(3) linkage isomers cannot be made.

H-bonding in **4** (cf. supplementary material) is as follows: The molecules form centrosymmetric dimers via two N(1)···O(2) contacts of 2.82(3) Å. This feature rules against O(4) as being the site of the acidic proton of the uracil. O(4) is H bonded to the water molecule O(1W) (2.74(3) Å) and the latter to the

---

(27) According to ^{1}H NMR, the yield of **4** is 60% under conditions described in the Experimental Section. We note that the isolated yield after single gel chromatography was much lower though.

(28) Lippert, B. *J. Raman Spectrosc.* **1979**, *8*, 274.

(29) (a) Berners-Price, S. J.; Frenkiel, T. A.; Frey, U.; Ranford, J. D.; Sadler, P. J. *J. Chem. Soc., Chem. Commun.* **1972**, 789, and references cited. (b) Slightly different pK_a values have also been reported: Miller, S. E.; House, D. A. *Inorg. Chem.* **1991**, *187*, 125.

(30) For discussion regarding this aspect, see: Singh, C. *Acta Crystallogr.* **1965**, *19*, 861.

(31) Taylor, R.; Kennard, O. *J. Mol. Struct.* **1982**, *78*, 1.

(32) Lock, C. J. L.; Pilon, P.; Lippert, B. *Acta Crystallogr.* **1979**, *B35*, 2533.

Table 7. Selected Interatomic Distances (Å), Angles (deg), and Hydrogen-Bonding Interactions for **4**[a]

	Distances		
Pt(1)–Cl(1)	2.280(9)	Pt(1)–N(11)	2.028(19)
Pt(1)–N(3)	2.038(19)	Pt(1)–N(10)	1.999(19)
C(4)–N(3)	1.32(3)	C(4)–O(4)	1.21(3)
C(4)–C(5)	1.50(3)	N(3)–C(2)	1.34(3)
O(2)–C(2)	1.22(3)	N(1)–C(6)	1.35(3)
N(1)–C(2)	1.39(2)	C(5)–C(6)	1.32(3)
	Angles		
N(3)–Pt(1)–N(10)	86.8(7)	N(11)–Pt(1)–N(10)	92.0(7)
N(11)–Pt(1)–N(3)	176.8(7)	Cl(1)–Pt(1)–N(10)	178.4(5)
Cl(1)–Pt(1)–N(3)	93.4(6)	Cl(1)–Pt(1)–N(11)	87.9(6)
Pt(1)–N(3)–C(4)	116.7(14)	Pt(1)–N(3)–C(2)	117.2(15)
O(4)–C(4)–C(5)	119(2)	N(3)–C(4)–C(5)	117.2(19)
N(3)–C(4)–O(4)	123.8(19)	C(4)–N(3)–C(2)	125.6(19)
C(6)–N(1)–C(2)	123(2)	C(4)–C(5)–C(6)	116(2)
N(1)–C(6)–C(5)	122(2)	O(2)–C(2)–N(1)	119(2)
N(3)–C(2)–N(1)	115(2)	N(3)–C(2)–O(2)	126(2)
	Possible Hydrogen Bond Distances ≤3 Å		
O(4)–O(1W)[f]	2.74(3)	O(4)–N(10)[d]	2.98(2)
O(2)–N(1)[b]	2.82(3)	N(10)–O(4)[c]	2.98(2)
N(11)–O(4)[c]	2.98(3)	O(1W)–O(2W)[e]	2.71(3)
O(2W)–O(2)	2.58(3)		
	Possible Hydrogen Bond Angles		
C(4)–O(4)–O(1W)[f]	141.7(15)	C(4)–O(4)–N(10)[d]	143.8(14)
C(2)–O(2)–N(1)[b]	124.5(15)	Pt(1)–N(10)–O(4)[c]	104.7(8)
Pt(1)–N(11)–O(4)[c]	103.9(8)	C(2)–N(1)–O(2)[b]	116.8(16)

[a] Symmetry operations. [b] $-x, -y, -z$. [c] $x, 1/2 - y, -1/2 + z$. [d] $x, 1/2 - y, 1/2 + z$. [e] $1 - x, 1 - y, -z$. [f] $-x, 1 - y, 1 - z$.

Table 8. Comparison of Ring Dimensions in Calix[4]arene and Metal Analogues as Given in Chart 2

sites	calix[4]arene[a]	Pt_4[b]	Pt_4Ag_4[c]
1⋯3′	2.53	2.86	2.90
7⋯7‴	5.07	5.87	5.81
3⋯1″	5.99	5.31	5.02
3′⋯1‴			7.45
7′⋯7‴	7.19	8.26	8.28

[a] Cone conformation; averaged values; ref 35. [b] 1,3-Alternate conformation. [c] Pinched-cone conformation.

second water molecule O(2W) (2.71(3) Å) which in turn H bonds (2.58(3) Å) to O(2).

Abstraction of the Cl ligand in **4** by Ag^+ in aqueous solution gives the corresponding aqua complex *cis*-$[(NH_3)_2Pt(UH\text{-}\mathit{N3})(H_2O)]^+$. As judged by ^1H NMR spectroscopy and potentiometric titration, the solution behavior of this species is very much different from that of *cis*-$[a_2Pt(UH\text{-}\mathit{N1})(H_2O)]^+$ ($a = NH_3$ or a_2 = en). In the ^1H NMR spectrum of an aqueous solution of the former (pD raised to 5–6 with NaOH), two additional sets of uracil resonances grow in with time. Without addition of OH^- (pD ≃ 4), only one new set of forms. The behavior is qualitatively similar to that of *cis*-$[(NH_3)_2Pt(1\text{-}MeU\text{-}\mathit{N3})(H_2O)]^+$.[33] As in this case, we assign the two new resonances to a head–tail dimer, *cis*-$[(NH_3)_2Pt(UH\text{-}\mathit{N3})]_2^{2+}$, and a μ-hydroxo dimer, *cis*-$\{[(NH_3)_2Pt(UH\text{-}\mathit{N3})]_2(OH)\}^{3+}$, the latter formed in a pH range corresponding to the pK_a of the Pt aqua group (*vide infra*) and the head–tail dimer preferentially in moderately acidic medium.

This interpretation is supported by results of a potentiometric titration study: Unlike in the case of $[(en)Pt(UH\text{-}\mathit{N1})(H_2O)]^+$, where the titration curve drastically changes upon aging and protons are released during this process,[9] the titration curve of a sample of *cis*-$[(NH_3)_2Pt(UH\text{-}\mathit{N3})(H_2O)]^+$ changes relatively little with time (supplementary material). Moreover, the titration curve does *not* give any indication for a substantial release of H_3O^+ upon aging. However, the consumption of base for the process

$$\mathit{cis}\text{-}[(NH_3)_2Pt(UH\text{-}\mathit{N3})(H_2O)^+] \xrightarrow[-H_2O]{+OH^-} \mathit{cis}\text{-}(NH_3)_2Pt(UH\text{-}\mathit{N3})(OH)$$

is only 82% if a monomeric structure is assumed. The second end point (deprotonation of UH at N(1)) is not observed. The pK_a (after addition of 1.5 × 0.82 = 1.23 equiv of NaOH) can be estimated to be 11.5, very much as in related compounds.[34] This behavior is interpreted in terms of a partial (9%) head–tail dimerization of the monomer according to

$$2\mathit{cis}\text{-}[(NH_3)_2Pt(UH\text{-}\mathit{N3})(H_2O)]^+ \xrightarrow{-2H_2O} \mathit{cis}\text{-}[(NH_3)_2Pt(UH\text{-}\mathit{N3},O)_2Pt(NH_3)_2]^{2+}$$

Relative ^1H NMR intensities (H(5), H(6) resonances), obtained from spectra of comparable concentrations to those used in the titration work, agree well with this picture.

The pK_a of the aqua ligand in *cis*-$[(NH_3)_2Pt(UH\text{-}\mathit{N3})(H_2O)]^+$, which is 7.2, is higher by a factor of 10 as compared to that of $[(en)Pt(UH\text{-}\mathit{N1})(H_2O)]^+$ or *cis*-$[(NH_3)_2Pt(UH\text{-}\mathit{N1})(H_2O)]^+$. Thus, very much in contrast to **1**, the aqua complex of the uracil–N(3) linkage isomer does not undergo any spectacular cyclization reaction under conditions comparable to the formation of **2**. Reasons for this significant difference deserve further investigations.

Comparison with Calix[4]arenes. The cyclic tetramer $[(en)Pt(UH\text{-}\mathit{N1,N3})]_4(NO_3)_4$ (**2**) and its deprotonated form(s) can be considered analogues of the fully organic calix[4]arenes. As compared to these, the following similarities and differences exist: (i) The isolated complex **2** adopts a 1,3-alternate conformation in the solid state. Calix[4]arenes in general prefer the cone conformation, but rim functionalization can occasionally lead to a freezing out of the 1,3-alternate conformer.[23] In aqueous solution, **2** is conformationally flexible, however, with the cone conformer being the other major species. (ii) Coordinating cations affect the conformer equilibria: Ag^I coordination via O(2) oxygens appears to greatly stabilize the cone form, while *cis*-a_2Pt^{II} ($a = NH_3$ or a_2 = en) stabilizes the 1,3-alternate form.[24] (iii) The principal difference between **2** and classical calix[4]arenes is the linkage entity, which is N–Pt–N in **2** but C–C–C in the calix[4]arenes (cf. Chart 3). As a consequence of the different angles at the bridging entity (C, ~104°; Pt, ~90°) and of different bond lengths (N–Pt *vs* C–C), geometries of the cavities of calix[4]arenes[35] and of **2** also differ (Table 8, Chart 2). More significant than these differences in geometry is the fact that due to the 90° angles about Pt, the ring system in **2** is clearly less flexible. (iv) The affinity of **2** for cations appears to be, despite its 4-fold positive charge, higher than in the case of calix[4]arenes. Apart from the Pt_4Ag_4 species **3**, four additional Pt^{II} entities have been added to **2** to give octanuclear complexes.[24] Binding of additional electrophiles primarily is a consequence of the high basicity of the exocyclic oxygens of the N-platinated uracil rings, very much as in the related 1-methyluracil and 1-methylthymine systems.[25,36] (v) Preliminary studies on the interaction of **2** with organic anions strongly suggest that **2** in its cone conformation acts as a host.[37] In general, calix[4]arenes do not display this property. We propose that the positive charge of the metal analogue **2** as compared to underivatized calix[4]arenes explains this difference.

Outlook. The synthesis and structural characterization of a metal analogue of a classical calix[4]arene opens the way to a class of macrocyclic ring systems comprised of nucleobases (or

---

(33) Lippert, B.; Neugebauer, D.; Raudaschl, G. *Inorg. Chim. Acta* **1983**, *78*, 161.

(34) (a) Inagaki, K.; Kidani, Y. *Bioinorg. Chem.* **1978**, *9*, 157. (b) Pfab, R.; Jandik, P.; Lippert, B. *Inorg. Chim. Acta* **1982**, *66*, 193.

(35) See, e.g.: Andreetti, G. D.; Pochini, A.; Ungaro, R. *J. Chem. Soc., Perkin Trans. 2* **1983**, 1773.

(36) Lippert, B. In *Handbook of Nucleobase Complexes*; Lusty, J. R.; Ed.; CRC Press: Boca Raton, FL, 1990; Vol. I, pp 9–46.

(37) Rauter, H.; Lippert, B., unpublished results

suitable heterocycles in general) and bridging metal entities. Our present findings suggest that a host–guest chemistry similar to that of the classical calixarenes can be established, which involves binding of cations, anions, and small neutral molecules. The possibility to use metals of different coordination geometries simultaneously,[38] and the variation in heterocyclic ligands provide a rich potential for future synthetic work.

While compound **2** does not represent the first example of a cyclic nucleobase complex,[39] host–guest studies appear not to have been the aim of this work. A similar approach to ours, the use of a cyclic Pd^{II}, 4,4′-bipyridine complex for recognition of organic molecules in water, has been reported.[40]

With regard to our interest in Pt uracil chemistry in general, the synthesis of open oligomers of defined size via ring-opening reactions of **2** is another goal of future work.

Acknowledgment. This work was supported by the Deutsche Forschungsgemeinschaft, DFG, and the Fonds der Chemischen Industrie. We thank Ms. Heike Meuer, University of Bochum, for collection of the X-ray data set of **1**, Dr. S. Menzer and Mrs. Anette Danzmann for recording NMR spectra, and Mr. M. Lutterbeck for preparation of some of the schemes.

Supplementary Material Available: Tables of anisotropic thermal parameters ^{1}H NMR spectra of **1**, view of cation of **3**, stereoview of crystal packing of **1** and **4**, packing of **2**, and pH titration of *cis*-$[(NH_3)_2Pt(UH\text{-}N3)(H_2O)]^+$ (8 pages); tables of observed and calculated structure factors for **1**, **2**, and **4** (23 pages). This material is contained in many libraries on microfiche, immediately follows this article in the microfilm version of the journal, and can be ordered from the ACS; see any current masthead page for ordering information.

---

(38) Jaworski, S.; Menzer, S.; Lippert, B.; Sabat, M. *Inorg. Chim. Acta* **1993**, *205*, 31.

(39) (a) Lorberth, J.; El-Essawi, M.; Massa, W.; Labib, L. *Angew. Chem., Int. Ed. Engl.* **1988**, *27*, 1160. (b) Uchida, K.; Toyama, A.; Tamura, Y.; Sugimura, M.; Mitsumori, F.; Furukawa, Y.; Takeuchi, H.; Harada, I. *Inorg. Chem.* **1989**, *28*, 2067. (c) Smith, D. P.; Baralt, E.; Morales, B.; Olmstead, M. M.; Maestre, M. F.; Fish, R. H. *J. Am. Chem. Soc.* **1992**, *114*, 10647.

(40) Fujita, M.; Yazaki, J.; Ogura, K. *J. Am. Chem. Soc.* **1990**, *112*, 5645.